Jpn J Radiol (2013) 31:706–712
DOI 10.1007/s11604-013-0233-5

CASE REPORT

Fibrolamellar hepatocellular carcinoma with biliary tumor thrombus: an unreported association

Anna Maria De Gaetano · Erida Nure · Ugo Grossi · Francesco Frongillo · Rosellina Russo · Fabio Maria Vecchio · Maria Carmen Lirosi · Gabriele Sganga · Carla Felice · Lorenzo Bonomo · Salvatore Agnes

Received: 5 April 2013 / Accepted: 2 July 2013 / Published online: 13 July 2013

Abstract Fibrolamellar hepatocellular carcinoma (FHCC) is a rare malignant tumor of hepatocyte origin occurring earlier in life than typical hepatocellular carcinoma (HCC). We describe a distinctive case of FHCC with biliary tumor thrombus (BTT) in a 25-year-old Caucasian patient, pointing out the imaging features supported by histopathology.

Keywords Fibrolamellar hepatocellular carcinoma (FHCC) · Hepatocellular carcinoma (HCC) · Biliary tumor thrombus (BTT)

Introduction

Fibrolamellar hepatocellular carcinoma (FHCC) is a rare malignant tumor of hepatocyte origin that differs from hepatocellular carcinoma (HCC) in etiology, demographics, condition of the affected liver, and tumor markers. FHCC usually occurs in young adults lacking a background of chronic liver disease and other risk factors for HCC. Clinical and laboratory findings are usually nonspecific and jaundice is a rare sign [1, 2]. Imaging studies are of major importance in clinical diagnosis and distinct radiological features have been identified [3, 4]. Use of percutaneous biopsy is appropriate in cases of uncertain radiologic diagnosis [5]. In published reports, most investigators emphasized the relatively indolent course and good prognosis of FHCC [1] compared with typical HCC, although data on treatment and prognosis are scarce [6]. Aggressive surgical liver resection with extended lymphadenectomy or liver transplantation may be indicated for postoperative recurrence [7]. We describe a unique case of FHCC in a 25-year-old man, presenting as a hepatic mass with biliary invasion and a bile duct tumor thrombus. To the best of our knowledge, this is the first report of FHCC with biliary tumor thrombus (BTT).

Case report

A 25-year-old Caucasian male patient was admitted with abdominal pain and obstructive jaundice. He had no significant past medical history nor previous medication, nor history of concomitant use of any drug or alcohol intake. He had a family history for colorectal cancer (father). Physical examination revealed abdominal tenderness in the mid-epigastric region extending to the left flank. Both liver and spleen were normal at palpation. Blood pressure, temperature, and heart and respiratory rates were also within normal range.

Laboratory studies indicated normal complete blood count, serum protein electrophoresis, and renal function with abnormal serum levels of alanine aminotransferase

A. M. De Gaetano · R. Russo · L. Bonomo
Department of Bio-Sciences and Radiological Imaging, Catholic University of the Sacred Heart, Rome, Italy

E. Nure · U. Grossi (✉) · F. Frongillo · M. C. Lirosi · G. Sganga · S. Agnes
Department of Surgery, Transplantation Service, Catholic University of the Sacred Heart, Largo A. Gemelli, 8, 00168 Rome, Italy
e-mail: grossiugo@gmail.com

F. M. Vecchio
Department of Pathology, Catholic University of the Sacred Heart, Rome, Italy

C. Felice
Department of Internal Medicine, Catholic University of the Sacred Heart, Rome, Italy

(115 U/L), cholesterol (219 mg/dL), direct bilirubin (2.86 mg/dL), gamma-glutamyl transferase (84 U/L), and alkaline phosphatase (749 U/L). Levels of alpha-fetoprotein (AFP), carbohydrate antigen (CA) 19–9, and carcinoembryonic antigen (CEA) were within the normal range. Tests for hepatitis viruses showed anti-HAV, HBsAg, HBeAg, anti-HBe, anti-HBc, HBV DNA, and anti-HCV were negative, and anti-HBs were positive, because of vaccination.

Abdominal ultrasound revealed a hepatic solitary lobulated mass with dishomogeneous echotexture measuring 85 mm in transverse diameter (Fig. 1). The lesion was located in the left lobe and was associated with a diffuse marked intrahepatic bile ducts dilatation, predominantly in the right lobe.

Computed tomography (CT) scan was performed in the arterial, portal, and venous phases, after infusion of a nonionic iodinated contrast medium (370 mgI/mL), with a 64-detector CT scanner (LightSpeed VCT; GE Healthcare, WI, USA). Nonenhanced CT scan confirmed an isoattenuating hepatic mass with lobulated margins and central calcifications (Fig. 2a); contrast-enhanced arterial-phase CT scan revealed irregular heterogeneous enhancement of the lesion (Fig. 2b). Contrast-enhanced portal venous and equilibrium-phase CT scans showed increasing homogeneity of the tumor with visualization of a central scar. Intrahepatic bile ducts dilatation was confirmed and enlarged lymph nodes were visualized at the hepatic hilum.

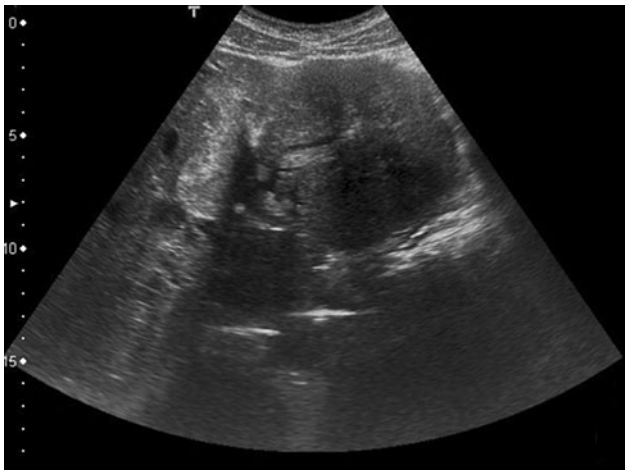

Fig. 1 Transverse ultrasound scan reveals an 85-mm isoechogenic mass with lobulated margins in the left liver lobe

Magnetic resonance imaging (MRI) was performed on a 1.5 T system (Signa Horizon; GE Healthcare, WI, USA) with an 8-channel phased-array body coil. Dynamic imaging was performed after administration of gadobenate dimeglumine (MultiHance; Bracco) at a dose of 0.1 mmol/kg body weight of the 0.5 M solution followed by 20-mL saline flush (0.9 %) at a flow rate of 2.5-mL/s, using a power injector. MultiHance is an hepatobiliary contrast agent; approximately 3–5 % of the injected dose is taken up by functioning hepatocytes and excreted in bile, enabling hepatobiliary or delayed phase imaging (DPI) of the liver. MR imaging confirmed a 9 cm lobulated mass in liver segments 2 and 3, hypo intense on T1-weighted images and hyperintense on T2-weighted images with fibrous scar hypointense on both pulse sequences (Fig. 3a, b). Heterogeneous enhancement of the tumor was observed in the arterial phase; this became progressively more homogeneous on delayed images. An hypointense central scar with delayed enhancement was clearly detectable (Fig. 3c, d).

The mass invaded the biliary tract with secondary marked dilatation (Fig. 4a); magnetic resonance cholangiography (MRCP) revealed a tumor thrombus growing continuously into the segmental intrahepatic ducts and extending through the left hepatic duct to the common bile

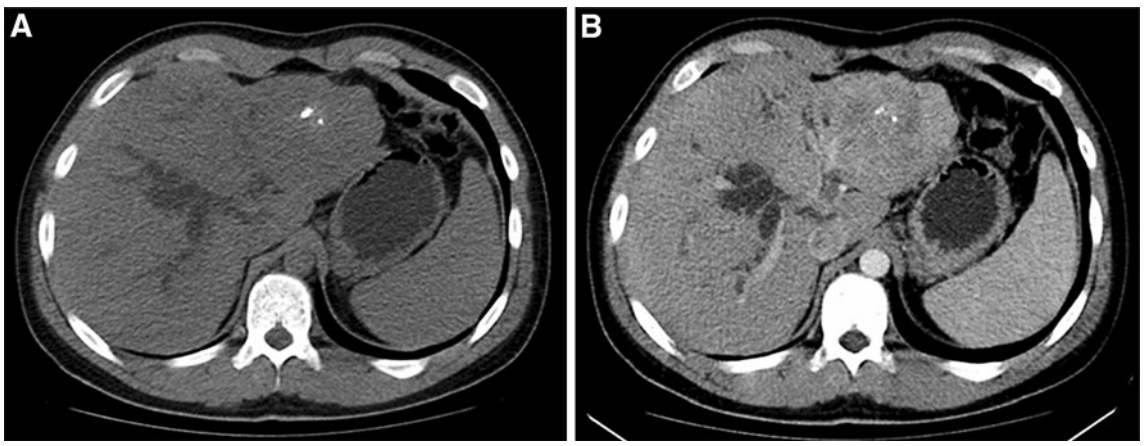

Fig. 2 Nonenhanced CT scan shows a large iso-attenuating mass in the left liver lobe. Central calcifications are clearly visible. Dilatation of intrahepatic bile ducts is present in the right liver lobe (**a**). Contrast-enhanced arterial-phase CT scan shows inhomogeneous enhancement of the tumor and confirms bile ducts dilatation (**b**)

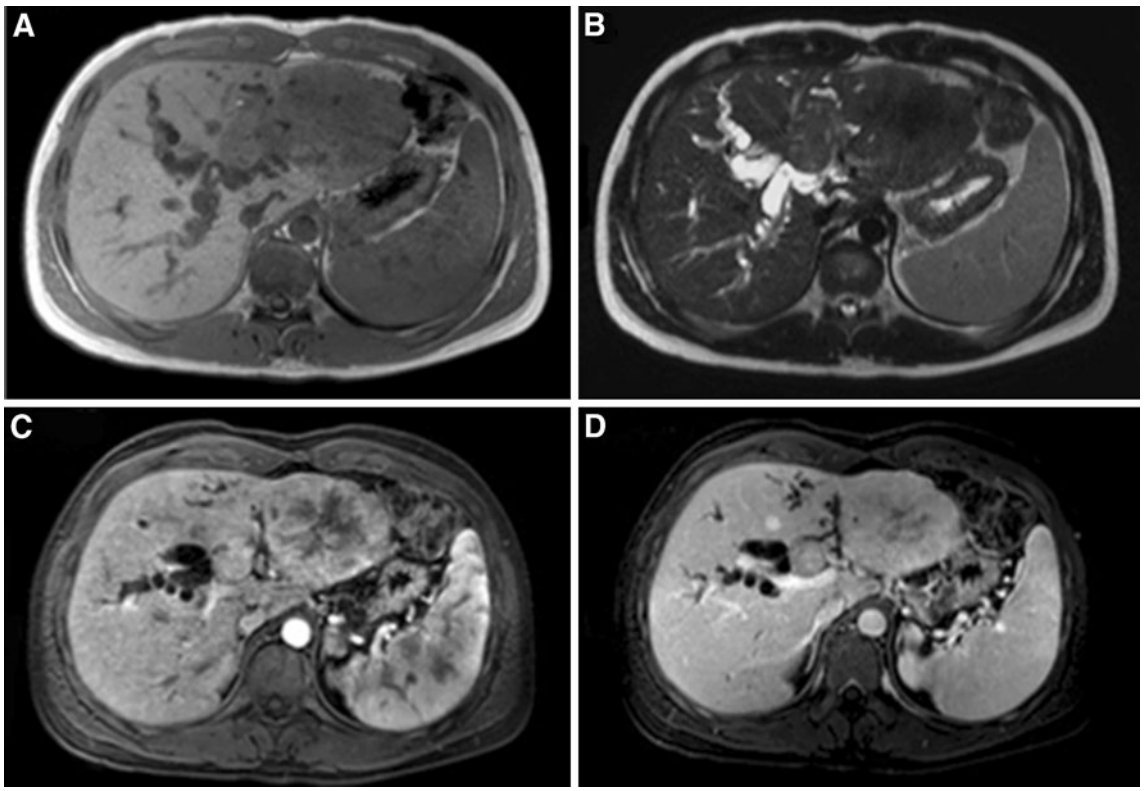

Fig. 3 A breath-hold transverse T1-weighted in-phase 2D fast spoiled gradient echo (2D FSPGR) sequence (TR/TE, 180/4.4–2.2; flip angle, 80°; FOV, 48 × 48 cm; matrix, 256 × 224; section thickness, 7 mm; slice spacing, 1 mm) shows a slightly hypointense mass in liver segments 2 and 3 (**a**). A breath-hold transverse T2-weighted fast-recovery fast spin-echo (FRFSE) sequence (eco train length, 17; FOV 48 × 48 cm; matrix, 256 × 224; section thickness, 7 mm; slice spacing, 1 mm) with a frequency-selective fat-suppression technique shows a heterogeneous isointense mass with a hypointense central scar. Both sequences reveal tumor extension towards the hepatic hilum and bile duct infiltration with dilatation of the right intrahepatic ducts (**b**). On gadolinium-enhanced T1-weighted gradient-echo images obtained in arterial (**c**) and portal venous phases (**d**), the mass heterogeneously enhances during the early phase and becomes increasingly homogeneous in the portal phase. On both images a hypointense central scar is evident. Bile duct involvement is confirmed

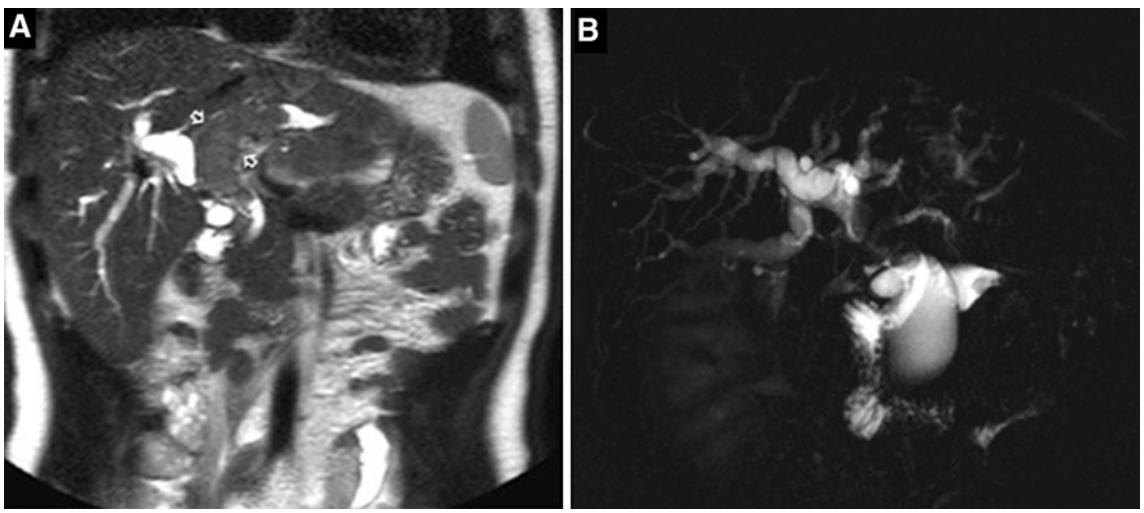

Fig. 4 Coronal T2-weighted fat-suppressed spin-echo MR image shows bile duct dilatation and a tumor thrombus growing continuously into the segmental intrahepatic ducts extending through the left hepatic duct to the main bile duct (*between the two empty arrows*) (**a**). MRCP imaging shows dilatation of intrahepatic bile ducts of both lobes and a filling defect from the left hepatic duct to the middle common bile duct with disruption of the main biliary confluence (**b**)

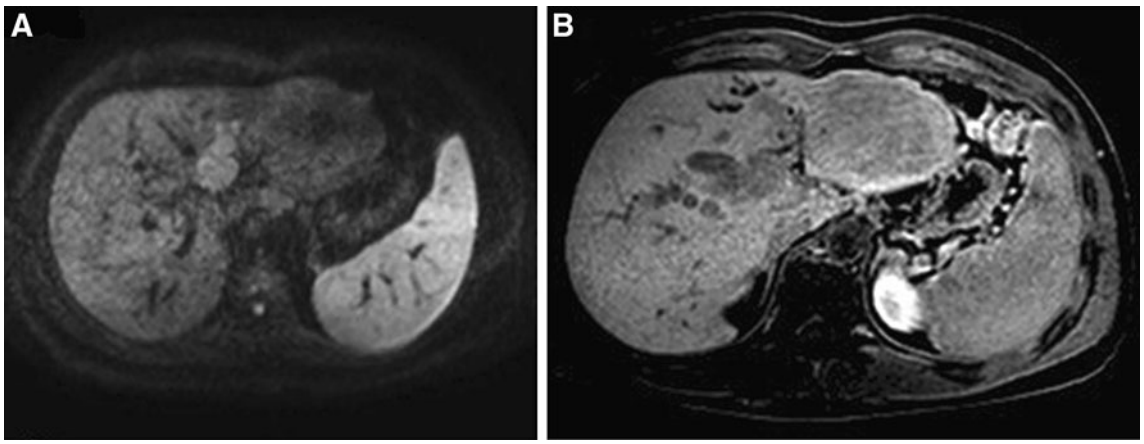

Fig. 5 Dynamic imaging was performed after administration of gadobenate dimeglumine (MultiHance®) at a dose of 0.1 mmol/kg body weight of the 0.5 M solution followed by 20-mL saline flush (0.9 %) at a flow rate of 2.5-mL/s, using a power injector. Imaging in the pre contrast, arterial (approximately 30 s), portal (approximately 50 s), equilibrium (approximately 180 s), and delayed (90–120 min) phases was performed by use of a T1-weighted breath-hold transverse 3D fast spoiled gradient-echo (LAVA; Liver Acquisition with Volume Acceleration; GE Healthcare) sequence with fat suppression (TR/TE, 3.1/1.5; flip angle, 13°; bandwidth, 83.3 KHZ; FOV, 48 × 48 cm; matrix, 256 × 224; effective section thickness, 3.8 mm with no gap). Axial diffusion-weighted image (TR/TE, 4,500 ms/min; and b–800 s/mm^2) shows high signal intensity of the tumor thrombus and isointensity of the primitive mass (**a**). On delayed T1-weighted GRE images after administration of gadobenate dimeglumine the primary tumor and the biliary thrombus appear slightly hypointense 1.5 h after contrast material enhancement (**b**)

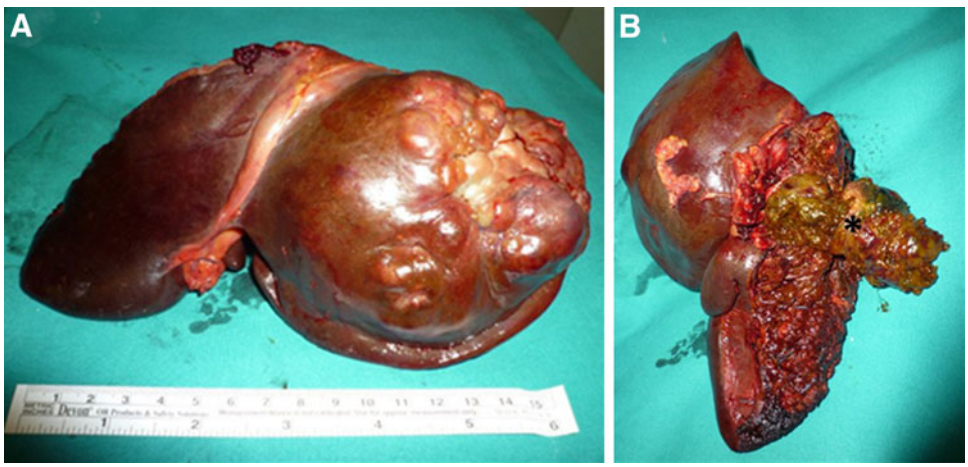

Fig. 6 The resected liver specimen contained a large lobulated left-lobe mass (**a**). Carcinoma was seen growing into the major hepatic duct and a tumor thrombus (*asterisk*) was present (**b**)

duct (Fig. 4b). Biliary hemorrhage was also detected by MR imaging; an hyperintense clot was apparent on T1-weighted images. Infiltration of the left portal vein and left hepatic artery was also present. The mass and the tumor thrombus appeared slightly hypointense on delayed T1-weighted GRE images after administration of gadobenate dimeglumine (MultiHance®) and slightly hyperintense on DWI imaging (b 800) (Fig. 5). ERCP revealed a defect from the left hepatic duct to the middle common bile duct with blood clots and disruption of the main biliary confluence.

All hepatic tumors that show a scar were considered in the differential diagnosis. For this reason, an ultrasound-guided percutaneous biopsy was performed from the left liver lobe; on histopathological analysis this revealed sheet-like proliferation of malignant hepatocytes, often interrupted with broad fibrous lamellar septa. The cells were immunoreactive with CD34 and hepatocyte paraffin 1 (Hep Par1), with inconsistent expression of cytokeratin 7. These findings enabled diagnosis of FHCC. Subsequently, the patient underwent left hepatic trisegmentectomy and lymphadenectomy. Tumor thrombus could be extracted and bile duct resection was not necessary. The postoperative course was uneventful. Histologic examination of the specimen confirmed the preoperative diagnosis. Gross examination of the resected liver specimen revealed a large lobulated left-lobe mass, rather hard and yellowish white, with a central scar. Carcinoma was seen growing into the common bile duct, often with erosion of the overlying surface biliary epithelium (Fig. 6). Surgical margin and hilar lymph nodes were negative for tumor. Microscopically, the tumor was a FHCC.

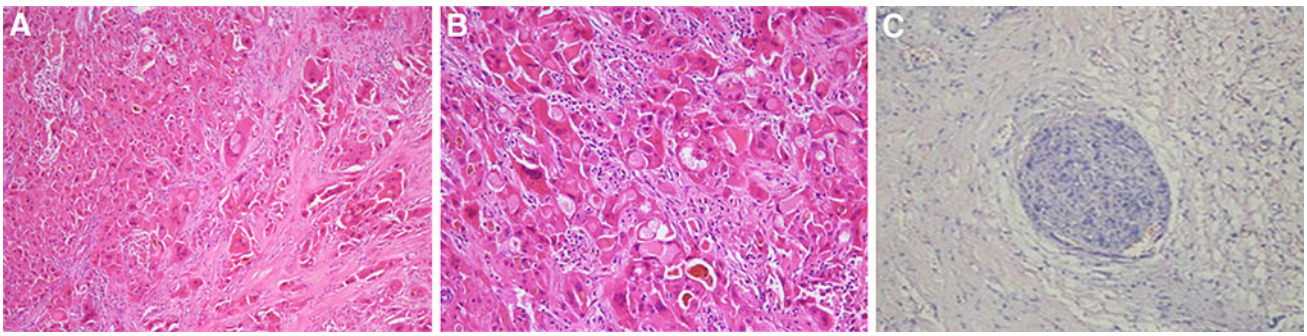

Fig. 7 Microscopic examination shows hepatocyte-like cells with granular eosinophilic cytoplasm arranged in sheets, cords, and trabeculae separated by fibrous stroma with parallel lamellae (**a**). Numerous intracytoplasmic pale inclusions are recognizable in neoplastic cells (**b**). Tumor cluster invasion into the bile duct wall is observed histologically (**c**)

The tumor was composed of hepatocyte-like cells with abundant granular eosinophilic cytoplasm and sometimes pale or hyaline cytoplasmic inclusions. Cells grew in sheets, cords, and trabeculae, occasionally in pseudoglands separated by abundant fibrous stroma arranged in parallel lamellae (Fig. 7). Subsequent follow-up was uneventful; 36 months after surgery there was no evidence of recurrence.

This study followed the ethical guidelines of our Institutional Review Board.

Discussion

Fibrolamellar hepatocellular carcinoma (FHCC) occurs predominantly in young adult patients, with an age range of 5–69 years and is equally likely in males and females. Most patients present in the second or third decade of life [1, 2]. Recently, Malouf et al. [8] differentiated pure FHCC, which typically occurs in patients aged <30 years, and often presents with lymph node metastasis and later extrahepatic recurrences, from mixed FHCC with HCC, which seems to resemble to classic HCC, occurring in patients aged >40 years and with the liver as the primary site of disease recurrence.

No specific risk factors for FHCC have been identified and typical risk factors for HCC such as viral hepatitis, alcohol abuse, and metabolic disease are absent. Unlike typical HCC, serum alpha-fetoprotein (AFP) is usually in the normal range [1, 2, 9].

Tumors are usually well circumscribed non-capsulated masses, characterized by well differentiated polygonal hepatic cells with eosinophilic and granular cytoplasm, surrounded by thick fibrous stroma arranged in bands; fibrotic lamellae often coalesce to form a central scar [3, 10, 11].

On radiologic images, FHCC typically appears as a large lobulated heterogeneous mass with a central scar in an otherwise normal liver. Combining clinical and laboratory data with radiologic imaging, correct diagnosis can often be suggested before performing biopsy that is indicated in cases of inconclusive findings from imaging [12, 13].

Although mostly presenting as a solitary mass (80–90 % of cases), FHCC may have small peripheral satellite lesions (10–15 %) or appear as a bilobed mass (5 %) or diffuse multifocal masses (<1 %) [1–3, 14].

The tumor is usually large at the time of diagnosis, ranging in size from 5 to 20 cm, with an average reported size of 13–14 cm. According to Ichikawa et al. [4] FHCC has lobulated margins in up to 65 % of cases. A central scar can be detected with contrast enhanced CT in 20–71 % of cases [4–13]. It is typically large and may be broad or stellate, eccentric or central. On delayed images, the scar often becomes hyperattenuating compared with the rest of the tumor, because of contrast material retention. Calcification is typical of FHCC, with reported incidence of 35–68 % [4–13]. Calcifications may be punctate, nodular, or stellate and are usually small (<5 mm), few (one to three in number), and almost always located near the center of the tumor [4].

The tumor enhancement pattern has been recognized as a useful differentiating feature. FHCC is almost always heterogeneous on unenhanced images, and heterogeneous enhancement is observed on hepatic arterial phase images. Tumor heterogeneity is related to its mixed content of neoplastic cells and fibrotic tissue and to intratumoral necrosis and hemorrhage [3, 4, 13–15]. The enhancement of FHCC becomes less heterogeneous and pronounced on portal venous and delayed-phase images.

On MR imaging the tumor is usually hypointense relative to the liver on T1-weighted images (86 % of cases) and hyperintense on T2-weighted images in the large majority (85 %) of cases [3]. If present, the fibrous scar is usually hypointense on all MR images, irrespective of the pulse sequence used [15, 16].

Differential diagnosis of FHCC includes all hepatic tumors with a scar [17], for example focal nodular

hyperplasia (FNH) and large hemangioma; scars are rarely seen in HCC, cholangiocarcinoma, and hepatic metastases.

It is important to distinguish FHCC from FNH and hemangioma because they usually require no treatment whereas FHCC requires aggressive surgical resection.

MR imaging with liver-specific contrast media is essential for differential diagnosis. On T2-weighted images, FNH usually has an hyperintense central scar whereas FHCC often has an hypointense scar [3].

Accurate differentiation of FNH from other hepatic tumors is achievable on delayed T1-weighted GRE images after administration of gadobenate dimeglumine (MultiHance®), because 1–3 h after contrast material enhancement FNH appears hyper-intense or iso-intense (96.9 %) [18].

Regional adenopathy occurs in 50–70 % of patients; distant metastases are less commonly detected (20 %). Invasion of hepatic vessels or bile ducts may be encountered in fewer than 5 % of cases [3, 4].

Although variable, the clinical presentation mostly includes the presenting signs and symptoms of typical HCC, for example abdominal pain, hepatomegaly, abdominal mass, weight loss, and anorexia. Jaundice is present in approximately 5 % of cases and results from biliary compression by direct tumor invasion, mass effect, or metastatic lymphadenopathy, rather than functional liver failure [19]. Although invasion of the portal vein or hepatic vein is a frequent finding in HCC, invasion of the bile ducts is quite uncommon; it is reported in 5–9 % of cases and mostly described for Asian patients with HBV infection [20].

The occurrence of biliary tumor thrombus (BTT) has never been associated to FHCC. Dynamic contrast-enhanced computed tomography (CT) and magnetic resonance imaging (MRI) are valuable diagnostic modalities to detect BTT. In such cases, the thrombus directly connects to the intrahepatic tumor. They both show typical HCC enhancement features in dynamic contrast-enhanced CT or MRI, including early enhancement in the hepatic arterial phase and rapid wash-out of contrast agent in the portal vein phase.

The presence of BTT makes differential diagnosis difficult, so fine-needle aspiration (FNA) is required. It is easily confused with Klatskin tumor or choledocholithiasis and has been described in HCC, peripheral cholangiocarcinoma, and metastatic tumors [20–22]. Primary mucosa-associated lymphoid tissue (MALT) lymphoma of the extrahepatic bile duct should also be considered in the differential diagnosis [23]. Biliary tract involvement in patients with HCC usually occurs in advanced stages owing to tumor compression or infiltration. The rare "icteric-type HCC" has been reported and is characterized by intraductal tumor growth. MRCP imaging is useful for diagnosis of biliary tumor thrombi and to evaluate the extension of thrombi and biliary hemorrhage.

In this report, the presence of a central scar and calcifications supported the diagnosis of FHCC, in contrast with intraductal growth of a neoplastic thrombus. This finding seemed to be associated with hypothetical more aggressive behavior of the tumor. In this case, however, it was not an absolute contraindication for surgical treatment, which resulted in 3-year recurrence-free survival.

Conflict of interest The authors declare that they have no conflict of interest.

References

1. Craig JR, Peters RL, Edmonson HA, Omata M. Fibrolamellar carcinoma of the liver: a tumor of adolescents and young adults with distinctive clinicopathologic features. Cancer. 1980;46:372–9.
2. Berman MM, Libbey NP, Foster JH. Hepatocellular carcinoma: polygonal cell type with fibrous stroma–an atypical variant with a favorable prognosis. Cancer. 1980;46:1448–55.
3. McLarney JK, Rucker PT, Bender GN, Goodman ZD, Kashitani N, Ros PR. Fibrolamellar carcinoma of the liver: radiologic-pathologic correlation. Radiographics. 1999;19(2):453–71.
4. IchikawaT, Federle MP, Grazioli L, Madariaga J, Nalesnik M, Marsh W. Fibrolamellar hepatocellular carcinoma: imaging and pathologic findings in 31 recent cases. Radiology. 1999;213(2):352–61.
5. Sarode VR, Castellani R, Post A. Fine-needle aspiration cytology and differential diagnoses of fibrolamellar hepatocellular carcinoma metastatic to the mediastinum: case report. Diagn Cytopathol. 2002;26(2):95–8.
6. Nagorney DM, Adson MA, Weiland LH, Knight CD, Smalley SR, Zinsmeister AR. Fibrolamellar carcinoma. Am J Surg. 1985;149:113–9.
7. Stipa F, Yoon SS, Liau KH, Fong Y, Jarnagin WR, D'Angelica M, et al. Outcome of patients with fibrolamellar hepatocellular carcinoma. Cancer. 2006;106(6):1331–8.
8. Malouf GG, Brugières L, Le Deley MC, Faivre S, Fabre M, Paradis V, et al. Pure and mixed fibrolamellar hepatocellular carcinomas differ in natural history and prognosis after complete surgical resection. Cancer. 2012;118(20):4981–90. doi:10.1002/cncr.27520.Epub2012Mar13.
9. Liu S, Chan KW, Wang B, Qiao L. Fibrolamellar hepatocellular carcinoma. Am J Gastroenterol. 2009;104(10):2617–24.
10. Vecchio FM. Fibrolamellar carcinoma of the liver: a distinct entity within the hepatocellular tumors. A review. Appl Pathol. 1988;6(2):139–48.
11. Vecchio FM, Fabiano A, Ghirlanda G, Manna R, Massi G. Fibrolamellar carcinoma of the liver: the malignant counterpart of focal nodular hyperplasia with oncocytic change. Am J Clin Pathol. 1984;81(4):521–6.
12. Smith MT, Blatt ER, Jedlicka P, Strain JD, Fenton LZ. Best cases from the AFIP: fibrolamellar hepatocellular carcinoma. Radiographics. 2008;28:609–13.
13. Brandt DJ, Johnson CD, Stephens DH, Weilan LH. Imaging of fibrolamellar hepatocellular carcinoma. AJR Am J Roentgenol. 1988;151:295–9.
14. Friedman AC, Lichtenstein JE, Goodman ZD, Fishman EK, Siegelman SS, Dachman AH. Fibrolamellar hepatocellular carcinoma. Radiology. 1985;157:583–7.

15. Corrigan K, Semelka RC. Dynamic contrast-enhanced MR imaging of fibrolamellar hepatocellular carcinoma. Abdom Imaging. 1995;20:122–5.
16. Titelbaum DS, Hatabu H, Schiebler ML, Kressel HY, Burke DR, Saul SH. Fibrolamellar hepatocellular carcinoma: MR appearance. J Comput Assist Tomogr. 1988;12:588–91.
17. Kim T, Hori M, Onishi H. Liver masses with central or eccentric scar. Semin Ultrasound CT MR. 2009;30(5):418–25.
18. Grazioli L, Morana G, Kirchin MA, Schneider G. Accurate differentiation of focal nodular hyperplasia from hepatic adenoma at gadobenate dimeglumine-enhanced MR imaging: prospective study. Radiology. 2005;236(1):166–77.
19. Soyer P, Roche A, Levesque M. Fibrolamellar hepatocellular carcinoma presenting with obstructive jaundice: a report of two cases. Eur J Radiol. 1991;13:196–8.
20. Gabata T, Terayama N, Kobayashi S, Sanada J, Kadoya M, Matsui O. MR imaging of hepatocellular carcinomas with biliary tumor thrombi. Abdom Imaging. 2007;32:470–4.
21. De Raffele E, Mirarchi M, Bassi F, Cola B. Hepatocellular carcinoma with neoplastic thrombosis of the common bile duct. Chir Ital. 2008;60:849–62.
22. Masuda N, Shiraishi Y, Okubo K, Okada T, Segawa T, Takada M, et al. A case report of renal cell carcinoma with metastatic intraductal tumor thrombus of the common bile duct. Hinyokika Kiyo. 2009;55(2):99–102.
23. Shito M, Kakefuda T, Omori T, Ishii S, Sugiura H. Primary non-Hodgkin's lymphoma of the main hepatic duct junction. J Hepatobiliary Pancreat Surg. 2008;15(4):440–3.